Wood, T.C., and P.S. Brummel. 2023. Hominin Baraminology Reconsidered with Postcranial Characters. In J.H. Whitmore (editor), *Proceedings of the Ninth International Conference on Creationism*, pp. 251-266. Cedarville, Ohio: Cedarville University International Conference on Creationism.

HOMININ BARAMINOLOGY RECONSIDERED WITH POSTCRANIAL CHARACTERS

Todd Charles Wood, and **PS Brummel**, Core Academy of Science, P.O. Box 1076 Dayton, TN 37321 USA, toddcharleswood@gmail.com, peter_brummel@yahoo.com

ABSTRACT

To date, hominin baraminology has been evaluated almost exclusively by craniodental characters, even though baraminology is ideally "holistic." Here, we present a new character set of 239 postcranial characters scored for fourteen taxa. The new matrix has 65.7% of its characters scored, which is comparable to existing craniodental character sets. We re-evaluated craniodental characters, postcranial characters, and a combined craniodental+postcranial character set using distance correlation and cluster analysis. Our results reveal that clustering with postcranial characters closely resembles clustering seen with craniodental characters or the combined character set. The only exception to this trend is *Australopithecus sediba*, which clusters with *Homo* taxa with craniodental characters but not with postcranial characters. Overall, however, our new characters provide excellent corroboration of previous baraminological analyses.

KEYWORDS

hominoids, primates, paleoanthropology, baraminology

INTRODUCTION

Initial baraminology studies of hominins identified the human holobaramin as members of the genus *Homo* together with *Au. sediba* (Wood 2010). Subsequent studies have reinforced this and recognized the recently discovered *Homo naledi* as human as well (Wood 2016, 2017). Only *Homo floresiensis* repeatedly fails to group with members of the human holobaramin (Sinclair and Wood 2021), despite a plausible case for their humanity based on behavioral considerations (Wise 2005). Aside from this anomaly, the repeated confirmation of the human holobaramin using multiple taxon and character samples makes the human holobaramin the most robustly identified holobaramin in all of baraminology.

In spite of this string of successes, hominin baraminology has been criticized from the beginning for including taxa in the human kind that critics believe do not belong (e.g., DeWitt 2010; Habermehl 2010; Menton 2010). O'Micks (2016) attempted to show that hominin baraminology did not support including *Homo naledi* or *Au. sediba* in the human holobaramin, but his analysis failed to properly account for sample size. His further attempts to perform baraminology on postcranial character matrices (O'Micks 2017a, 2017b) were not holistic, which weakens his conclusions. A more substantive critique came from Reeves (2021a, 2021b), wherein he exposed shortcomings in the methodology used to define the human holobaramin. Wood's response (2021) showed that the original methods, while questionable on a theoretical level, nevertheless agreed very well with more conventional cluster analysis methods, such as medoid partitioning and fuzzy analysis. Sinclair and Wood (2021) subsequently showed that the expanded set of clustering tools recommended by Reeves (2021b) actually supported including *Au. sediba* and the genus *Homo* (except *H. floresiensis*) in the human holobaramin.

That said, all previous hominin baraminology studies by Wood (2010, 2016, 2017; Sinclair and Wood 2021) were based only on craniodental characters. Thus, despite showing a clearly and robustly defined human holobaramin, the research was not truly holistic. One might argue that holism is too poorly defined to be of practical value in baraminology, but on a relative basis, holism has some merit. Considering only teeth or humeri or pelves is certainly less informative than considering an entire skeleton. While skulls are information dense (and for hominins, sometimes the only elements that are available), they give a more limited perspective on the human kind than considering characters from the entire body. This is especially important since creationists have long relied on the form of the entire skeleton to distinguish human from nonhuman (e.g., Hartwig-Scherer 1998; Lubenow 2004).

Previously, efforts to study postcranial material were hampered by the limited number of taxa for which postcranial material was known (Wood 2013) and by the availability of material for study. Significant advances in the past two decades have substantially altered this situation. Newly described taxa have been found alongside substantial skeletal material (Berger et al. 2010, 2015), and new discoveries have expanded our understanding of the skeleton of *Au. afarensis* (Haile-Selassie et al. 2010; Alemseged et al. 2006), *Au. africanus* (Clarke 2019a), and the Dmanisi hominins (Lordkipanidze et al. 2007). Further, highly detailed 3D scans have made many of these new discoveries publicly available, and other projects such as NESPOS (Groening et al. 2007) have made scans of previously discovered hominin fossils accessible to researchers. With these important new advances, creationists can now evaluate postcranial hominin characteristics more carefully than ever before.

To take advantage of these new resources and discoveries, we developed our own postcranial character matrix for hominins, from a combination of previously published character matrices, previously

published taxonomic descriptions, and original measurements and observations on digital scans and physical casts. These new characters were then analyzed using standard distance correlation and cluster analysis, as previously used in Wood (2021) and Sinclair and Wood (2021). The results are the most comprehensive analysis of hominin baraminology to date.

METHODS

Character matrix. An initial postcranial character list was assembled from published descriptions in Lordkipanidze et al. (2007), Berger et al. (2010), Senter (2010), Kivell et al. (2011), Arsuaga et al. (2015), Argue et al. (2017), Churchill and VanSickle (2017), Marchi et al. (2017), and Pugh (2022). Redundant characters from this list were removed, and new characters were developed from published literature descriptions. Finally, every character was evaluated based on direct examination of available skeletal evidence, and characters that could not be confirmed by inspection of scans, casts, or photographs were replaced with related characters. For all characters, character state 0 was reserved exclusively for the absence of a character state.

We selected fourteen taxa for our analysis based on the taxa included in the Wood (2020) character matrix. Our taxa include extant chimpanzees, gorillas, and humans, fossil taxa representing seven members of *Homo* (*H. erectus sensu lato*, *H. floresiensis*, *H. georgicus*, *H. habilis*, *H. heidelbergensis*, *H. naledi*, *H. neanderthalensis*), three members of *Australopithecus* (*Au. afarensis*, *Au. africanus sensu lato*, *Au. sediba*), and *Ardipithecus ramidus*. To maximize the number of scored character states, we opted to combine the African and Asian *H. erectus* taxa from Wood (2020) as a single taxon *H. erectus sensu lato*. In doing so, we retained the Dmanisi hominins as a separate taxon, here called *H. georgicus*. We also elected to include *Au. africanus* and Little Foot skeletal material in the taxon *Au. africanus sensu lato* rather than taking a position on the status of *Au. prometheus* (Berger and Hawks 2019; Clarke 2019b; Grine 2019). All taxonomic decisions here should be viewed only as pragmatic in order to maximize the number of character states rather than assessments of the merits of species descriptions and attributions.

To score additional postcranial character states and evaluate previously published postcranial character states, we consulted published photographs, specimen measurements and descriptions, 3D scans and prints, and physical casts. We also consulted original material for *Homo neanderthalensis* (Shanidar 3), *Australopithecus sediba* (MH1), and *Homo naledi* (LES-1) at public exhibits at the National Museum of Natural History in Washington D.C. and the Perot Museum of Nature and Science in Dallas, TX. Altogether, we directly scored 1,753 character states. The character matrix is available from Dryad (Wood and Brummel 2023).

In addition to this new matrix of postcranial characters, we used the Wood (2020) matrix of craniodental characters as a reference. In doing so, we eliminated taxa not included in the postcranial matrix, and we combined the African and Asian *H. erectus* into a single taxon. Where African and Asian *H. erectus* character states differed, we combined them as a polymorphism that included both character states. We also used the nonpolarized character coding that assigned character state 0 only to character states that were absent.

To combine the character matrices into a total evidence character matrix, we selected only craniodental characters with character relevance greater than 0.5 in order to balance the number of craniodental and postcranial characters and to prevent the analysis from being effectively weighted in favor of the craniodental characters. To do this, we eliminated characters 4, 7-10, 16-19, 30, 36, 44, 47-48, 51,

Table 1. Taxic relevance for each character set used in this study.

	All craniodental	High-relevance craniodental	Postcranial	Combined
Ardipithecus	0.205	0.296	0.222	0.259
Au. afarensis	0.675	0.811	0.778	0.795
Au. africanus s.l.	0.829	0.996	0.812	0.905
Au. sediba	0.376	0.490	0.724	0.606
Gorilla	0.798	0.951	0.983	0.967
H. erectus s.l.	0.954	0.996	0.649	0.824
H. floresiensis	0.322	0.449	0.603	0.583
H. georgicus	0.445	0.564	0.331	0.390
H. habilis	0.836	0.996	0.331	0.666
H. heidelbergensis	0.645	0.807	0.573	0.691
H. naledi	0.315	0.506	0.389	0.448
Neandertals	0.621	0.778	0.845	0.811
H. sapiens	0.893	0.996	0.975	0.985
Chimpanzee	0.749	0.926	0.979	0.952

54, 56, 59-62, 64, 68, 70, 74, 76, 80-81, 88, 92, 95, 99-100, 103-104, 107, 110-111, 123, 125, 132, 140-141, 147-151, 160-161, 165-166, 168, 170, 175, 181-182, 189-190, 192, 195, 206, 209-210, 212, 219, 224, 230-231, 235-238, 240, 243, 245, 247, 250-251, 254-256, 259, 264, 268-269, 281-282, 287, 295, 297-298, 301, 303-304, 306, 314-315, 318-319, 321, 326-328, 332, 335-338, 341-345, 350, 352, 358-359, and 362-391. As a result, we evaluated four different character matrices, the original craniodental character matrix reduced to the fourteen taxa here evaluated, a subset of high-relevance craniodental characters with character relevance $a > 0.5$, the postcranial characters, and a combined set of the high-relevance craniodental characters and all postcranial characters.

Baraminology analysis. Following Sinclair and Wood (2021), we used both simple matching (baraminic) distances and Jaccard distances for distance correlation and cluster analysis. We performed distance correlation analysis with both distance metrics as well as Pearson and Spearman correlations. We performed cluster analysis using medoid partitioning and fuzzy analysis with both types of distances. For each set of analyses, we used all characters present in the four character sets described above. All clustering and distance correlations calculations were done using BARCLAY (https://coresci.org/barclay). Any additional analyses were performed in R.

RESULTS

All craniodental characters. Before presenting and interpreting the postcranial characters and their clustering patterns, we sought to develop a comparison group of just craniodental characters for the fourteen taxa used in the postcranial character matrix. We derived this craniodental matrix from Wood's (2020) matrix by combining the Asian and African *Homo erectus* taxa into a single *Homo erectus s.l.*, as described in the methods. Because our previous analysis (Sinclair and Wood 2021) used a larger set of 17 taxa that included *H. rudolfensis* and *Au. anamensis*, in addition to separating African and Asian *H. erectus* into separate taxa, we performed all distance correlation and cluster analyses on just the present fourteen taxa to determine how the smaller taxon sample might alter previous results.

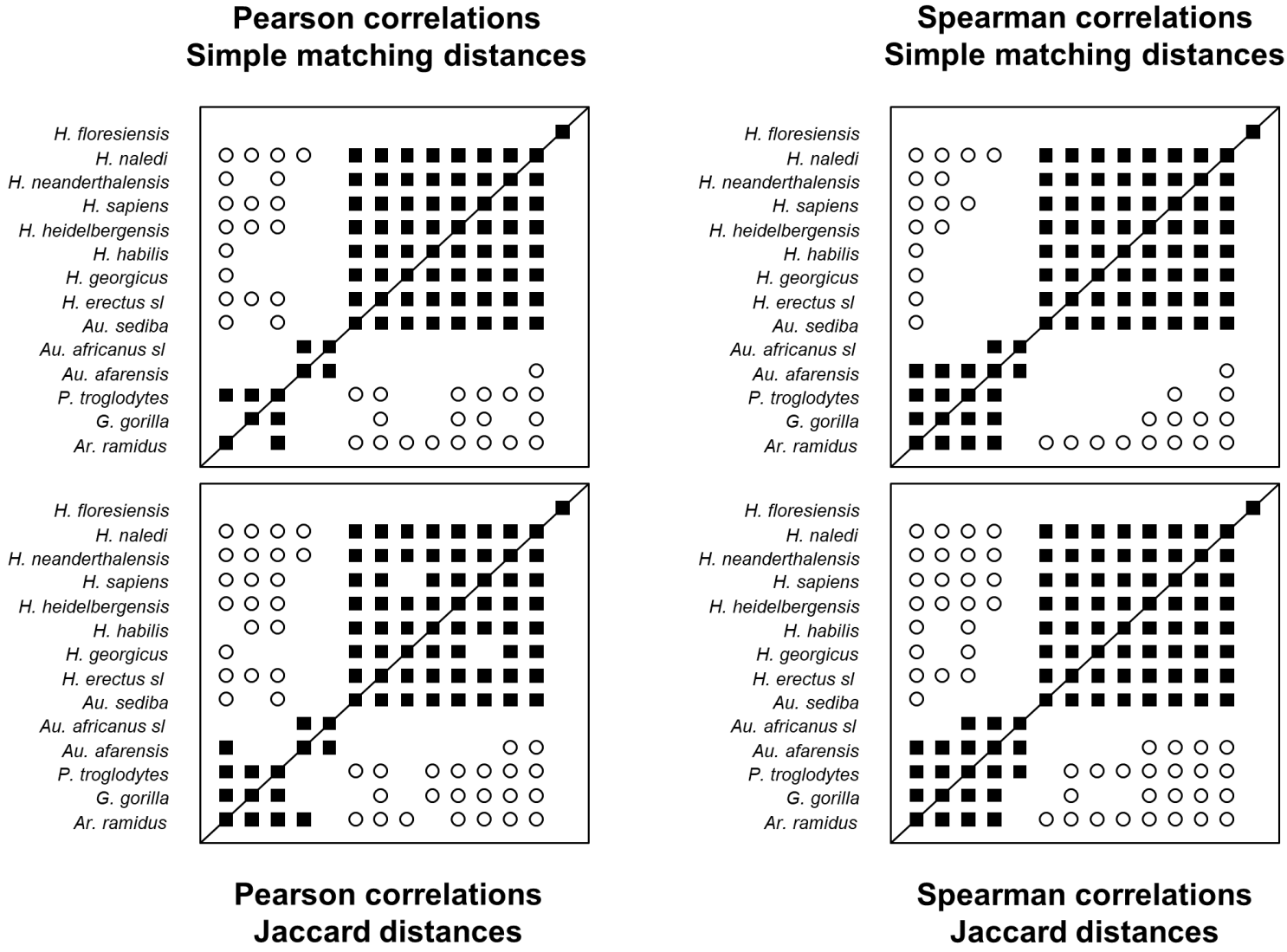

Figure 1. Distance correlation results for all craniodental characters. Correlations and distance metrics are shown in the diagram. Filled squares indicate significant, positive distance correlation. Open circles indicate significant, negative correlation.

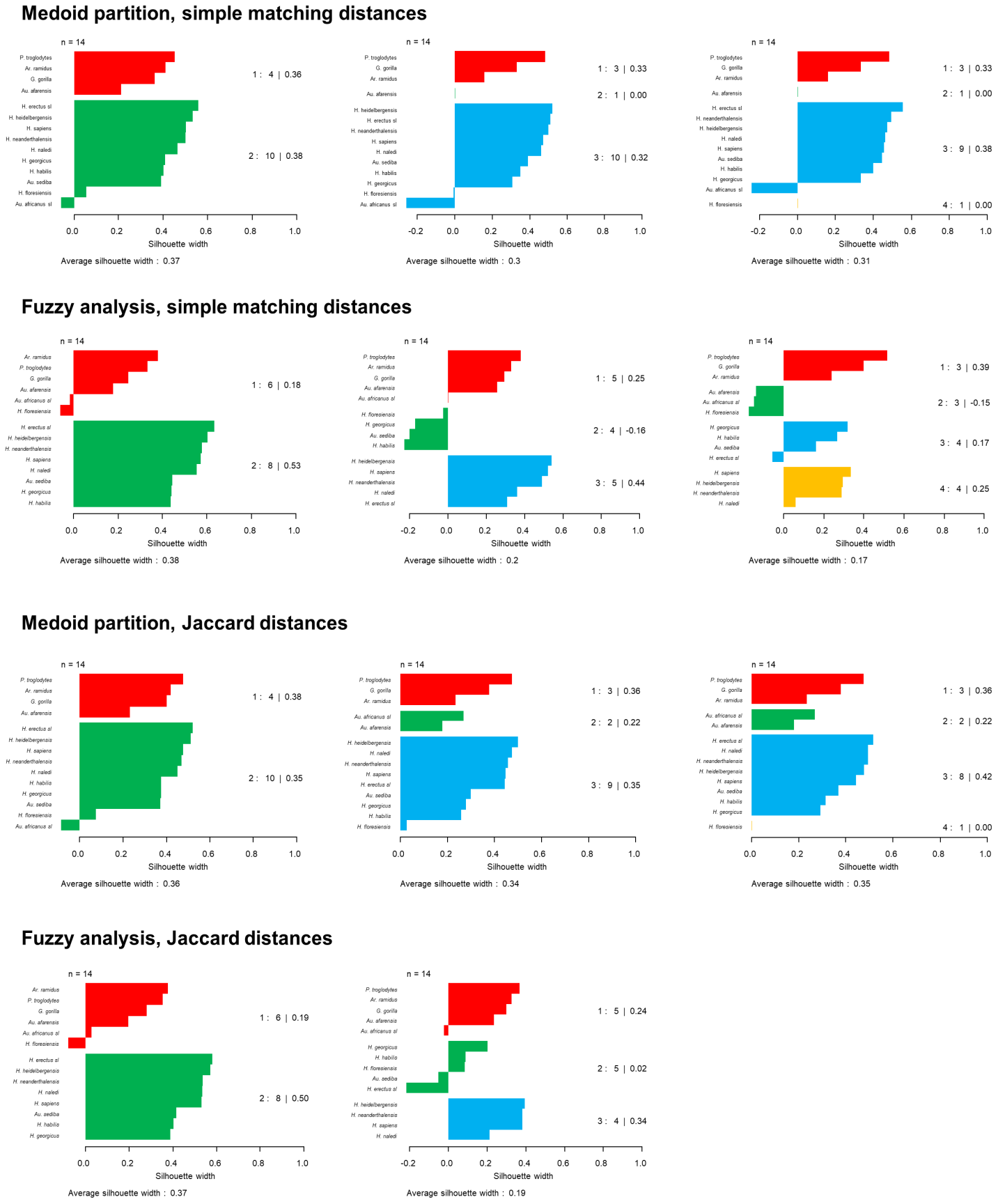

Figure 2. Silhouette plots for medoid partitioning and fuzzy analysis results for all craniodental characters. Cluster analysis type and distance metrics are shown in the diagram.

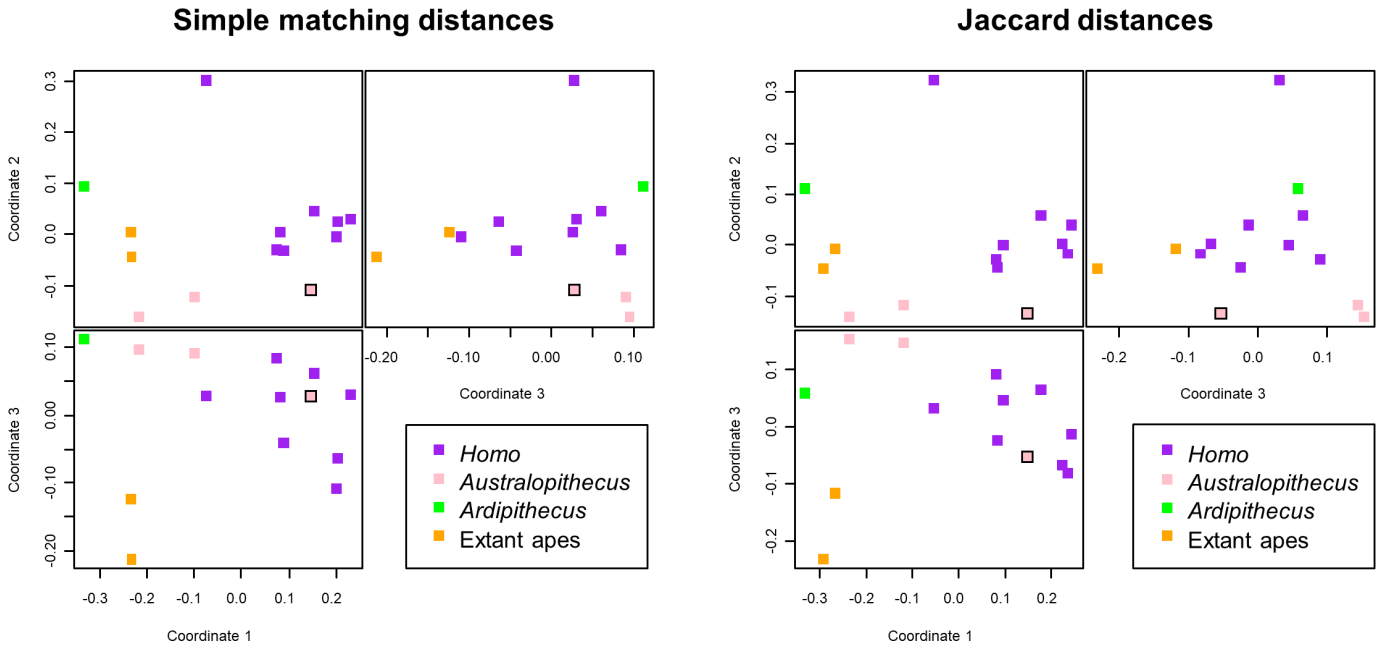

Figure 3. Orthogonal views of 3D MDS results for simple matching (left) and Jaccard distances (right) calculated from all craniodental characters. *Au. sediba* is indicated by a symbol with a black outline.

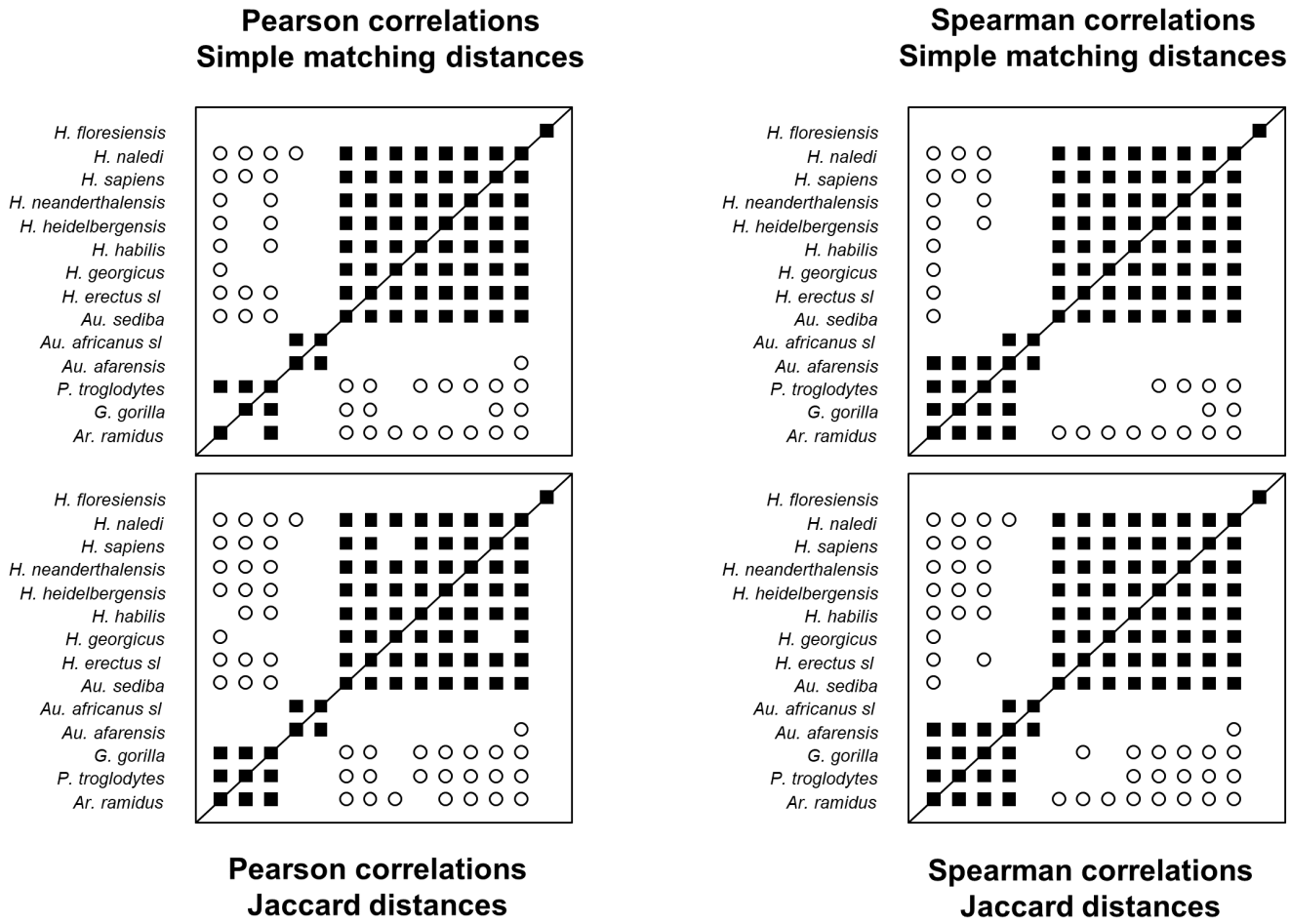

Figure 4. Distance correlation results for high-relevance craniodental characters. Correlations and distance metrics are shown in the diagram. Filled squares indicate significant, positive distance correlation. Open circles indicate significant, negative correlation.

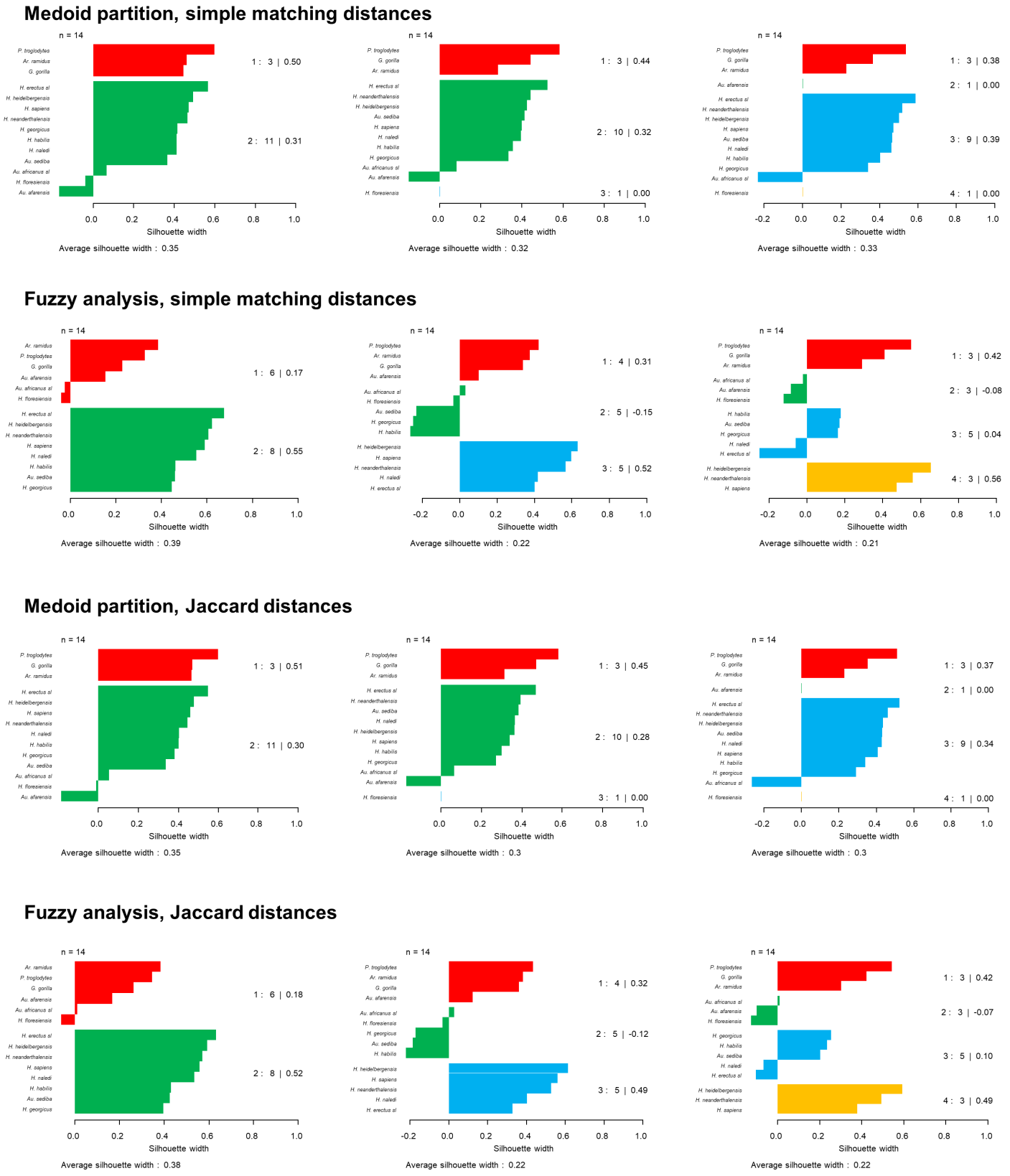

Figure 5. Silhouette plots for medoid partitioning and fuzzy analysis results for high-relevance craniodental characters. Cluster analysis type and distance metrics are shown in the diagram.

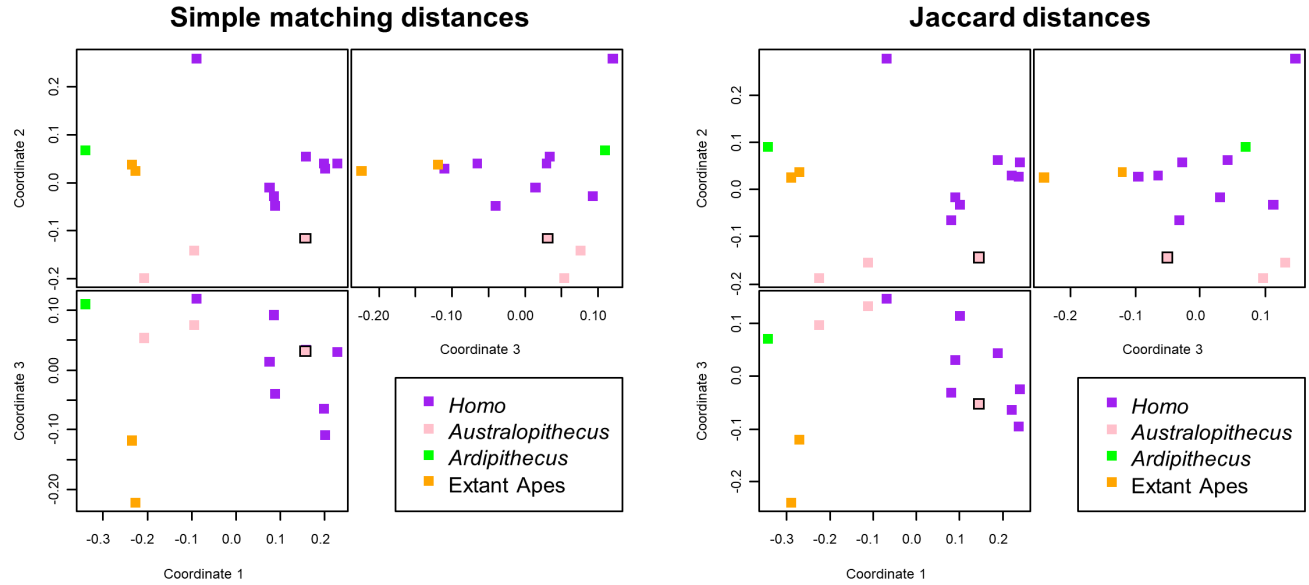

Figure 6. Orthogonal views of 3D MDS results for simple matching (left) and Jaccard distances (right) calculated from high-relevance craniodental characters. *Au. sediba* is indicated by a symbol with a black outline.

The full craniodental character matrix of 391 characters and 14 taxa has 5,474 possible character states, of which 3,387 are scored. The matrix is 61.9% complete. Character relevance ranges from 0.143 to 1, with a median of 0.571. Taxic relevance ranges from 0.205 (*Ar. ramidus*) to 0.954 (*H. erectus s.l.*), with a median of 0.660. Four taxa have taxic relevance less than 0.4 (*Ardipithecus*, *H. floresiensis*, *H. naledi*, and *Au. sediba*). See Table 1 for taxic relevance values for all taxa and character matrices.

Using these characters, we calculated simple matching and Jaccard distances with no character relevance filtering. Distance correlation results using both Pearson and Spearman correlations are shown in Figure 1. These results do not differ substantially from the previously published analysis (Sinclair and Wood 2021). A cluster of *Homo* taxa and *Au. sediba* is discernible, and the outgroup taxa cluster differently depending on the correlation type and the distance metric. *Homo floresiensis* displays neither significant positive nor negative correlation with any other taxa. There is extensive significant, negative correlation between the *Homo* + *Au. sediba* cluster and the outgroup taxa.

Cluster analysis of simple matching and Jaccard distances generally support the presence of a cluster containing *Homo* + *Au. sediba* (Figure 2). Curiously, medoid partitioning of simple matching distances consistently places *Au. africanus s.l.* in the *Homo* + *Au. sediba* clustering, but medoid partitioning with Jaccard distances places *Au. africanus s.l.* with *Au. afarensis* for $k > 2$. Average silhouette widths for all medoid partitions are greater than 0.3. The hard partition for two-cluster fuzzy analysis is identical for simple matching and Jaccard distances, and it places *Homo* taxa and *Au. sediba* in a single cluster, with *Homo floresiensis* in the outgroup cluster with chimpanzees and gorillas. The average silhouette widths for two-cluster fuzzy analysis with simple matching and Jaccard distances are 0.38 and 0.37 respectively. At higher cluster numbers, fuzzy analysis splits the *Homo* cluster using both simple matching and Jaccard distances, resulting in an average silhouette width of 0.2 or less.

The 3D MDS shows a cluster of *Homo* taxa with *Au. sediba* closely adjacent (Figure 3). This is the case for both simple matching and Jaccard distances. In both cases, chimpanzees and gorillas do not appear close to any australopiths or to *Ardipithecus*.

High-relevance craniodental characters. In order to create a combined character matrix that is roughly equally represented by craniodental and postcranial characters, we reduced the number of craniodental characters by removing characters with character relevance $a \leq 0.5$. The original craniodental character matrix contained 391 characters, which is 60% more characters than the 239 postcranial characters. By filtering for high relevance only, 243 craniodental characters were retained, which is nearly equal to the 239 postcranial characters. We used these high-relevance characters as a second craniodental comparison set for distance correlation and cluster analysis.

For 243 high-relevance craniodental characters and 14 taxa, there are 3,402 possible character states. With 2,566 character states scored, the matrix is 75.4% complete. Character relevance ranges from 0.571 to 1, with a median relevance of 0.786. Taxic relevance ranges from 0.296 (*Ar. ramidus*) to 0.996 (*H. erectus s.l.*, *H. habilis*, *H. sapiens*, and *Au. africanus s.l.*), with a median of 0.809 (Table 1). Only *Ardipithecus* has a taxic relevance less than 0.4.

Distance correlation results closely resembled those of the full craniodental matrix (Figure 4). Again, we see a cluster of *Homo* taxa and *Au. sediba*. *H. floresiensis* shares significant correlation with no other taxa. Correlations among the outgroup taxa vary by correlation type and distance metric. Significant, negative correlation is found between members of the *Homo* + *Au. sediba* cluster and the outgroup taxa.

Cluster analysis of the high-relevance craniodental characters also resembles that of the full craniodental character set (Figure 5). Medoid partitioning of the simple matching and Jaccard distances places *Au. africanus s.l.* consistently in the *Homo* + *Au. sediba* cluster,

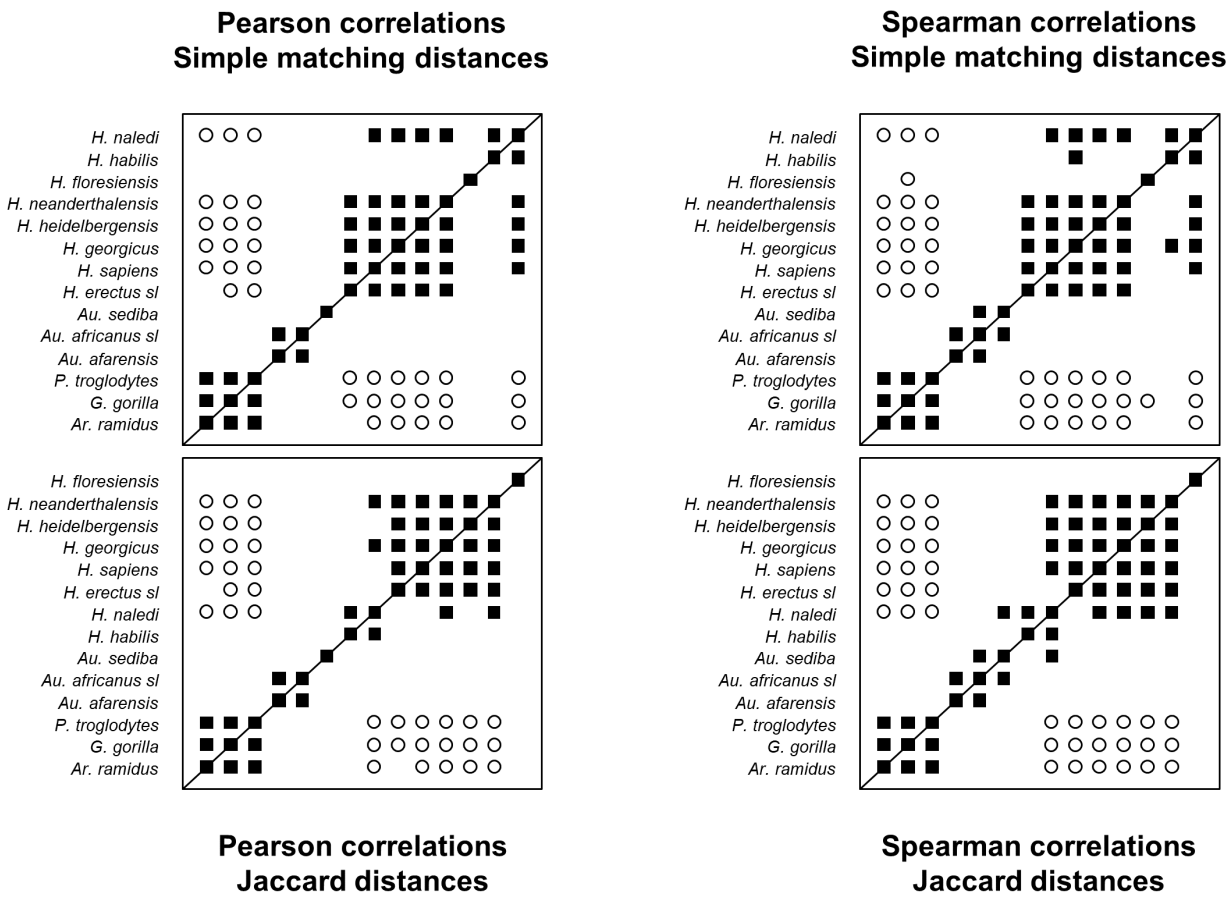

Figure 7. Distance correlation results for postcranial characters. Correlations and distance metrics are shown in the diagram. Filled squares indicate significant, positive distance correlation. Open circles indicate significant, negative correlation.

resulting in strongly negative silhouette widths for *Au africanus s.l.* and average silhouette widths between 0.3 and 0.35. In contrast, the two-cluster fuzzy analysis yielded a hard partition that placed *H. floresiensis*, *Au. africanus s.l.*, *Au. afarensis*, *Ardipithecus*, chimpanzee, and gorilla in a cluster separate from *Homo* + *Au. sediba* using both simple matching and Jaccard distances (average silhouette widths 0.39 and 0.38 respectively). At higher cluster numbers, fuzzy analysis again splits up the *Homo* + *Au. sediba* cluster, causing the average silhouette width to drop to 0.22 and below.

Unsurprisingly, the 3D MDS results closely resemble those of the full craniodental character matrix, with a cluster of *Homo* taxa closely adjacent to *Au. sediba* (Figure 6). Extant apes and the other two *Australopithecus* species are not particularly close to the *Homo* cluster nor to each other. These patterns are observed for MDS using both simple matching and Jaccard distances.

Postcranial characters. The postcranial character matrix contains 239 characters scored for 14 taxa. Of the 3,346 possible character states, 2,197 are scored, making the matrix 65.7% complete. Character relevance ranges from 0.214 to 1, with a median of 0.643. Taxic relevance ranges from 0.222 (*Ar. ramidus*) to 0.983 (gorilla), with a median of 0.687 (Table 1). Only four taxa have taxic relevance less than 0.4 (*Ar. ramidus*, *H. georgicus*, *H. habilis*, and *H. naledi*).

The distance correlation results using the postcranial characters closely resemble the distance correlation results using the craniodental characters (Figure 7). For both distance metrics and correlation types, there is a large cluster that consists of most of the *Homo* taxa. *Homo floresiensis* never shares significant distance correlation with any other taxa. Using Pearson correlations, *Homo habilis* only shares significant, positive distance correlation with *Homo naledi* in both distance metrics. Using Spearman correlations, *Homo habilis* shares significant, positive correlation with *Homo naledi* using Jaccard distances and with *Homo naledi* and *Homo georgicus* using simple matching distances. With Pearson correlations, *Au. sediba* also shares no significant, positive correlation with any other taxa using both simple matching and Jaccard distances. In contrast, *Au. sediba* shares significant, positive distance correlation with *Au. africanus s.l.* using Spearman correlations on simple matching distances. Using Spearman correlations on Jaccard distances, *Au. sediba* shares significant, positive correlation with both *Au. africanus s.l.* and *Homo naledi*. With all correlation types and distance metrics, chimpanzees, gorillas, and *Ar. ramidus* form a single cluster that shares significant, negative correlation with the members of the large *Homo* cluster.

Medoid partitioning produced the same clusters for both Jaccard and simple matching distances (Figure 8). With only two clusters, medoid partitioning placed all *Australopithecus* and *Homo* taxa in the same cluster, with chimpanzee, gorilla, and *Ardipithecus* in the

Medoid partition, simple matching distances

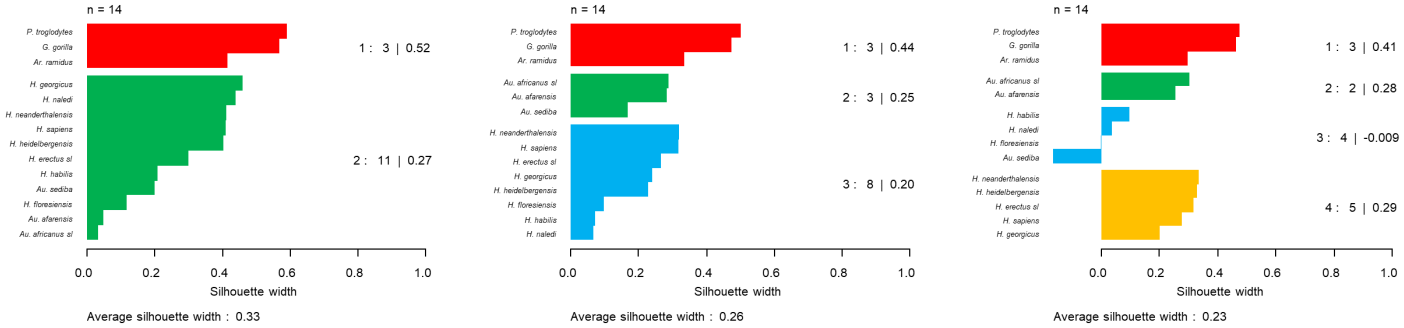

Fuzzy analysis, simple matching distances

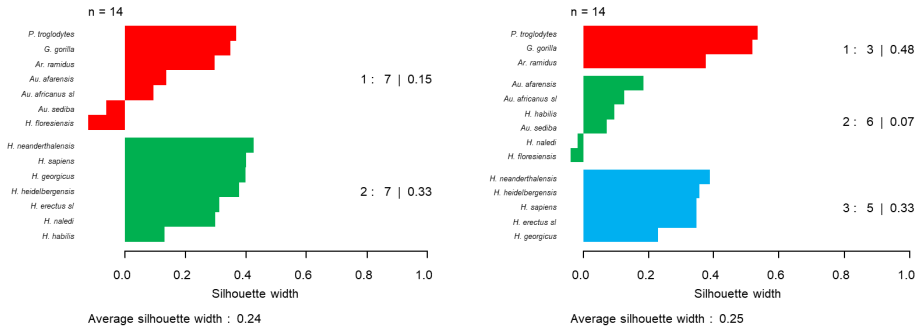

Medoid partition, Jaccard distances

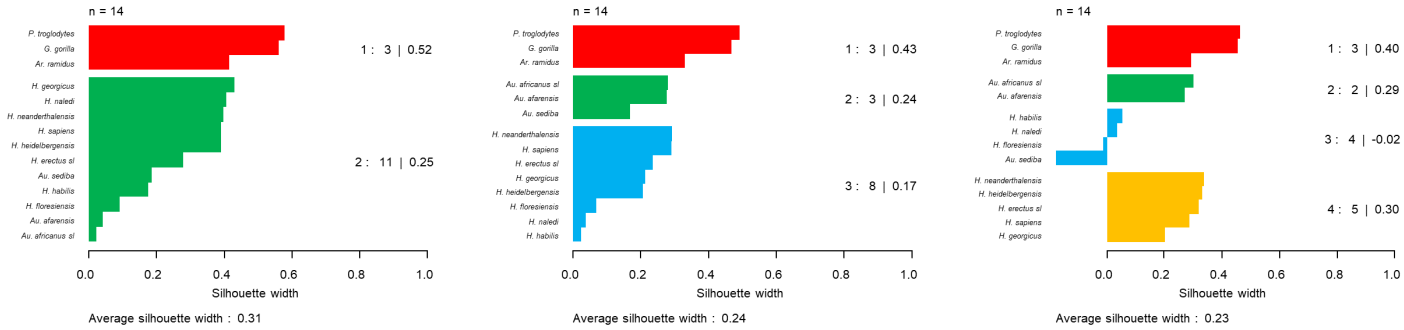

Fuzzy analysis, Jaccard distances

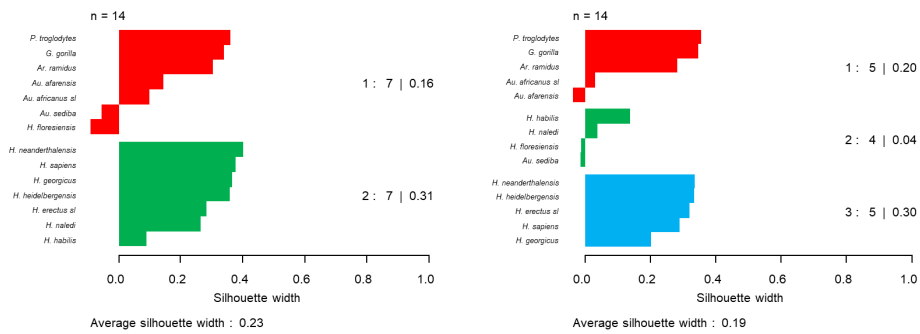

Figure 8. Silhouette plots for medoid partitioning and fuzzy analysis results for postcranial characters. Cluster analysis type and distance metrics are shown in the diagram.

other cluster. For three-cluster medoid partitioning, the clusters corresponded to all *Homo* taxa, all three *Australopithecus* taxa, and the remaining taxa. Four-cluster medoid partitioning divided up the *Homo* taxa and established a new cluster of *Homo* and *Au. sediba*.

Fuzzy analysis generated hard partitions for two clusters that evenly divided the taxa, placing all *Australopithecus* taxa and *Homo floresiensis* in the same cluster with chimpanzee, gorilla, and *Ardipithecus*. The other cluster contained the remaining *Homo* taxa. The same two clusters were observed with both simple matching and Jaccard distances. For three clusters, fuzzy analysis broke up the *Homo* taxa to make a cluster of *H. floresiensis*, *H. naledi*, *H. habilis*, and all three *Australopithecus* taxa for simple matching distances and a cluster of *H. habilis*, *H. naledi*, *H. floresiensis*, and *Au. sediba* for Jaccard distances. For both distance metrics, three-cluster fuzzy analysis recognized a cluster of *H. sapiens*, *H. neanderthalensis*, *H. heidelbergensis*, *H. erectus s.l.*, and *H. georgicus*. Distinguishing which clustering partition was best was difficult because the average silhouette widths for all medoid and fuzzy partitions were similar, ranging from 0.19 to 0.33.

The 3D MDS results differed from the craniodental MDS results (Figure 9). Most importantly, the *Homo* taxa are spread out more with postcranial characters than with craniodental characters. The dispersed *Homo* taxa can be observed with both simple matching and Jaccard distances. The second major difference is the position of *Au. sediba*. With craniodental characters, *Au. sediba* appears in the midst of the *Homo* taxa, but with postcranial characters, *Au. sediba* appears to be merely adjacent to the *Homo* taxa and just as close to other *Australopithecus* taxa as it is to the nearest *Homo* taxa. Otherwise, the chimpanzee, gorilla, and *Ardipithecus* appear to be closely adjacent to each other and distant from the *Homo* taxa. *Australopithecus afarensis* and *Au. africanus s.l.* also appear to be distant from the *Homo* taxa.

Combined character matrix. The combined character matrix of craniodental and postcranial data contains 482 characters, 49.6% of which are postcranial characters and 50.4% of which are craniodental characters. Of the 6,784 possible character states, 4,763 are scored, making the matrix 70.6% complete. Character relevance ranges from 0.214 to 1, with a median of 0.714. Taxic relevance ranges from 0.259 (*Ar. ramidus*) to 0.985 (*H. sapiens*), with a median of 0.743 (Table 1). Only two taxa have taxic relevance less than 0.4, *Ar. ramidus* and *H. georgicus*.

Distance correlation results show a clear cluster of *Homo* taxa with both correlation types and distance metrics, but individual distance correlations vary considerably between the Pearson and Spearman correlations (Figure 10). With Pearson correlations, *H. georgicus* shares significant, positive distance correlation with no other taxa and significant, negative correlation with both chimpanzee and gorilla. Using simple matching distances, *H. floresiensis* shares significant, positive distance correlation only with *H. habilis* and *H. erectus s.l.* Using Jaccard distances, *H. floresiensis* shares significant, positive distance correlation only with *H. erectus s.l.* With simple matching and Jaccard distances, *Au. sediba* shares significant, positive distance correlation only with *Homo naledi*. Using Spearman correlations, *H. georgicus* shares significant, positive distance correlation with all other *Homo* taxa, and *Au. sediba* shares significant, positive distance correlation with five *Homo* taxa, including *H. sapiens*. These patterns

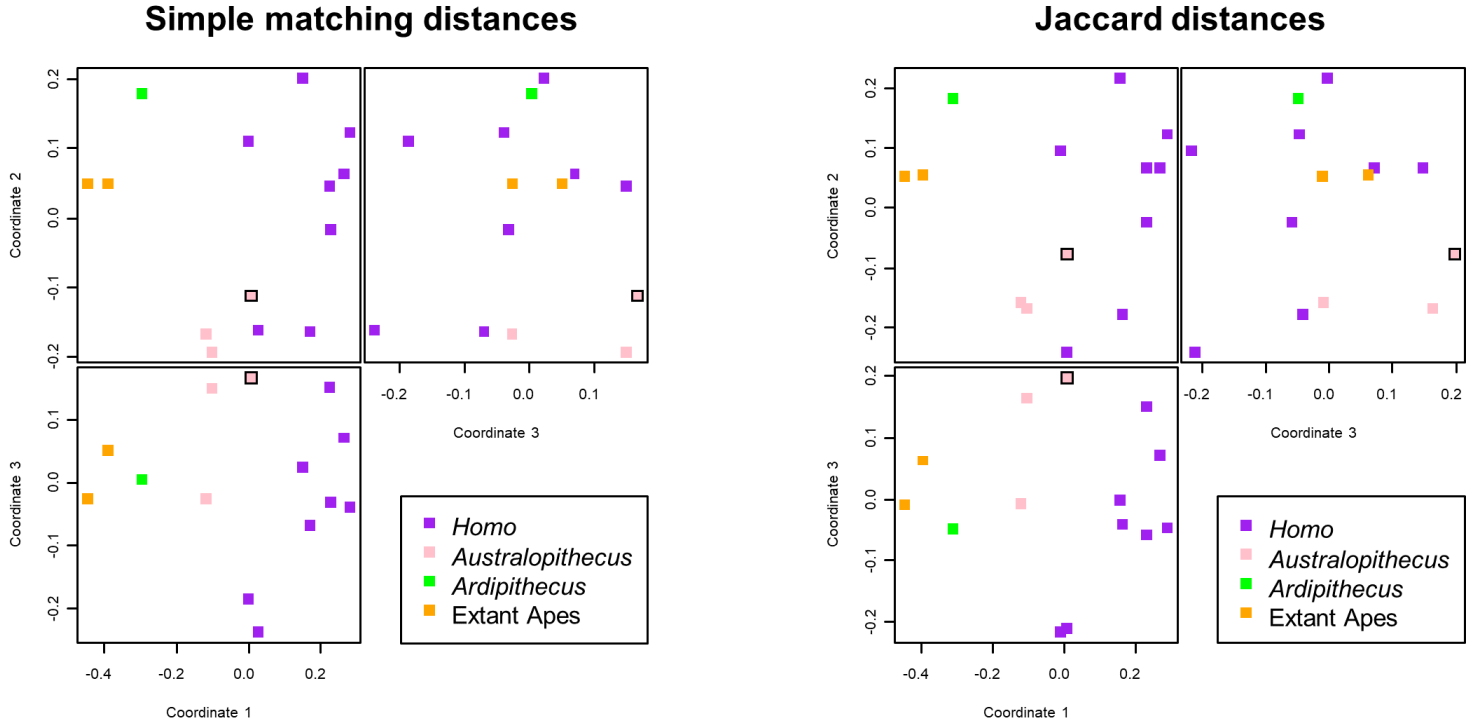

Figure 9. Orthogonal views of 3D MDS results for simple matching (left) and Jaccard distances (right) calculated from postcranial characters. *Au. sediba* is indicated by a symbol with a black outline.

are seen with both simple matching distances and Jaccard distances.

All medoid partitions are very similar when using simple matching or Jaccard distances (Figure 11). Medoid partitioning places chimpanzee, gorilla, and *Ardipithecus* in a single cluster for all cluster counts. With two clusters, all other taxa are placed in a single cluster, giving an average silhouette width of 0.35 for simple matching distances and 0.34 for Jaccard distances. At three clusters, *Au. africanus s.l.* and *Au. afarensis* are placed in a separate cluster, lowering the average silhouette width to 0.32 for simple matching distances and 0.3 for Jaccard distances. With four clusters, *Au. sediba* is separated from all other taxa into a singleton cluster, lowering the average silhouette width even further to 0.25 for simple matching distances and 0.23 for Jaccard distances.

The hard partition from two-cluster fuzzy analysis is nearly identical for both simple matching and Jaccard distances (Figure 11). In both cases, all *Homo* taxa are placed in a cluster with *Au. sediba*, and the remaining outgroup taxa are placed in the second cluster. The average silhouette width for this partition is 0.34 for simple matching distances and 0.32 for Jaccard distances. With three clusters, fuzzy analysis once again splits up the *Homo* + *Au. sediba* cluster, resulting in a drop in average silhouette width to 0.17 for simple matching distances and 0.15 for Jaccard distances.

The 3D MDS results resemble those of both craniodental matrices shown above, using both Jaccard and simple matching distances (Figure 12). There is a group of *Homo* in proximity to *Au. sediba*, and the other two *Australopithecus* lie at some distance from *Au. sediba*. Chimpanzee, gorilla, and *Ardipithecus* are not particularly close to one another and are at distance from the *Homo* group. The same patterns are seen with Jaccard and simple matching distances.

Clustering summary. Since the clusters from our analyses do not agree on the details, we evaluated the frequency that each pair of taxa clusters together in the 44 different cluster partitions from medoid partitioning, fuzzy analysis, and distance correlation using the high-relevance craniodental, postcranial, and combined character sets. Partitions of the full craniodental set were omitted from this assessment in order to prevent bias towards craniodental characters. Our results are shown in Table 2. We can see that the outgroup taxa chimpanzee and gorilla and *Ardipithecus* cluster together in all of our

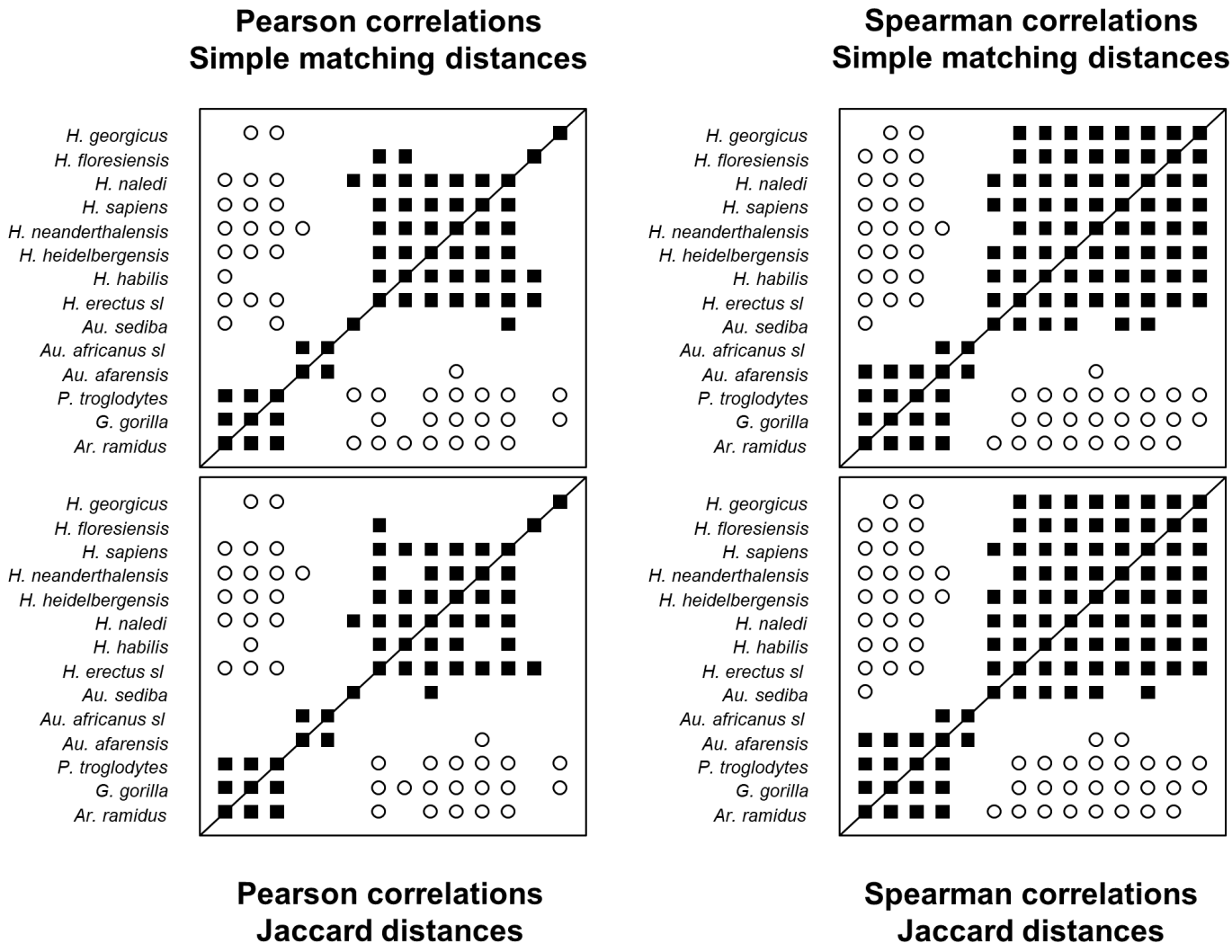

Figure 10. Distance correlation results for the combined character set. Correlations and distance metrics are shown in the diagram. Filled squares indicate significant, positive distance correlation. Open circles indicate significant, negative correlation.

Medoid partition, simple matching distances

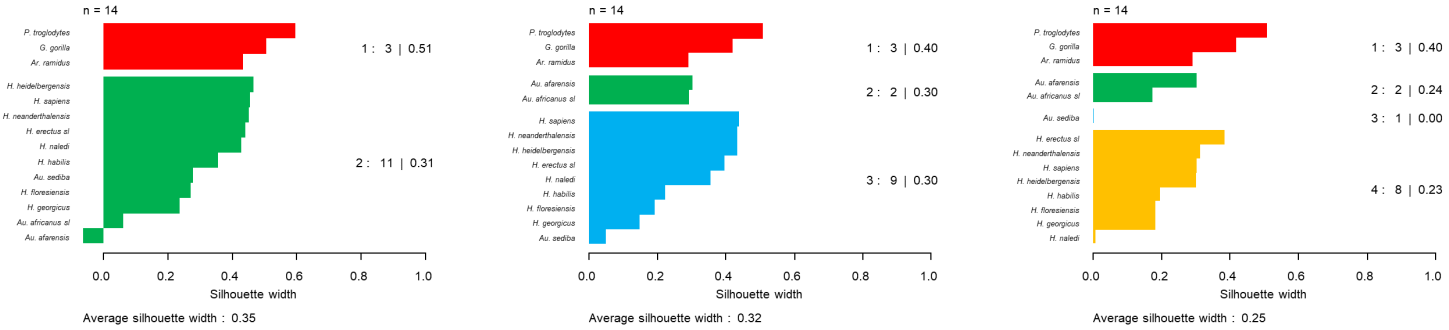

Fuzzy analysis, simple matching distances

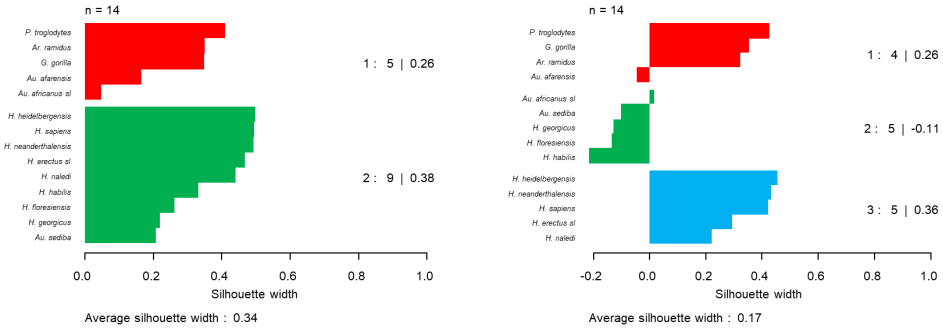

Medoid partition, Jaccard distances

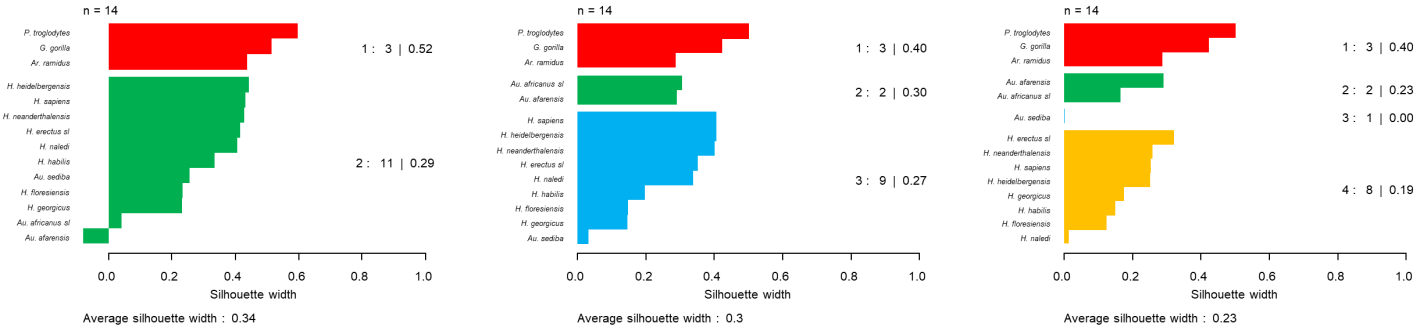

Fuzzy analysis, Jaccard distances

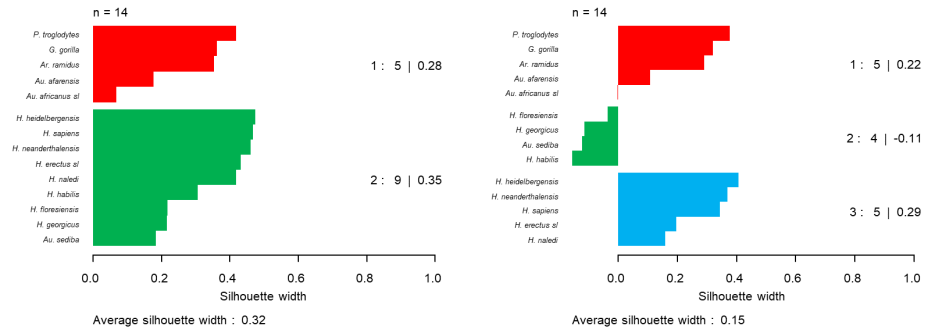

Figure 11. Silhouette plots for medoid partitioning and fuzzy analysis results for the combined character set. Cluster analysis type and distance metrics are shown in the diagram.

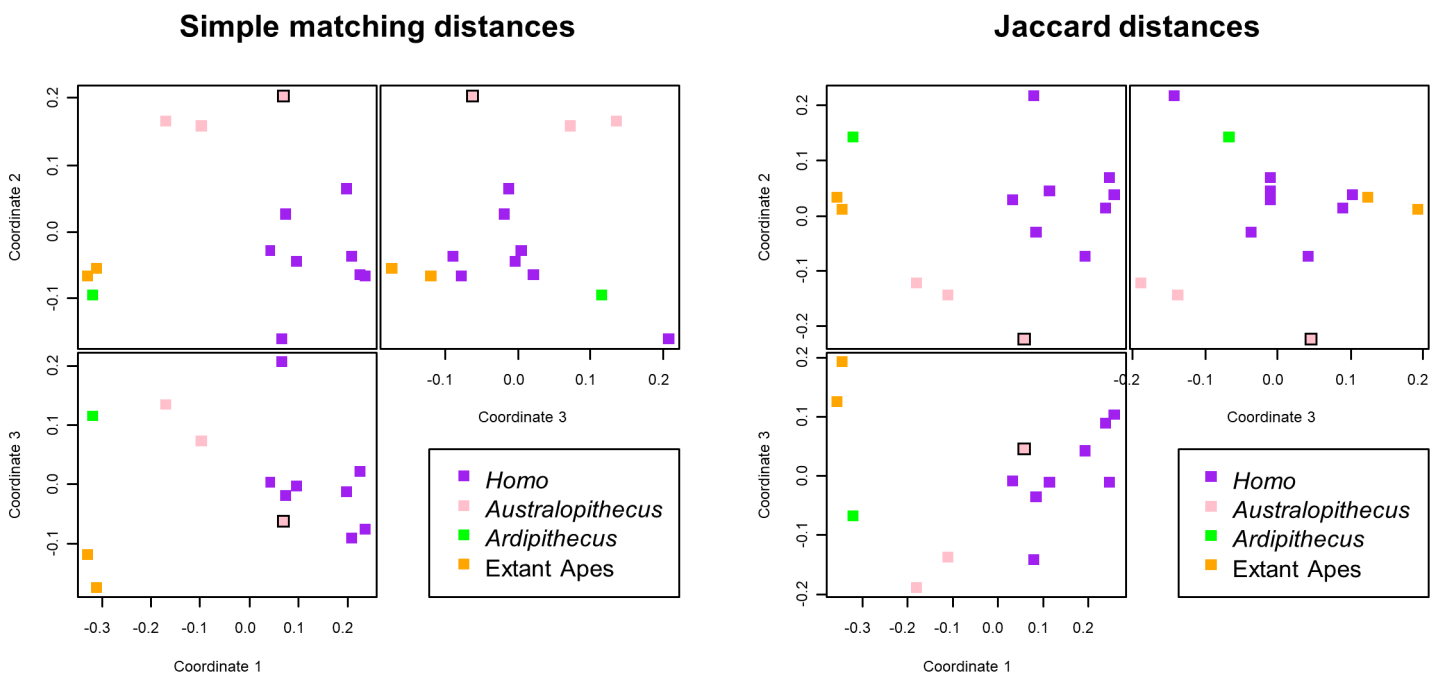

Figure 12. Orthogonal views of 3D MDS results for simple matching (left) and Jaccard distances (right) calculated from the combined character set. *Au. sediba* is indicated by a symbol with a black outline.

partitions. *Australopithecus africanus s.l.* clusters with *Au. afarensis* in 89% of the partitions, but *Au. africanus s.l.* clusters with *Au. sediba* in only 46% of our partitions. *Homo sapiens*, *H. erectus s.l.*, Neandertals, and *H. heidelbergensis* cluster together in at least 96% of all partitions. These four *Homo* taxa are analogous to the "Lubenow Core" of Ross et al. (2023), if we consider *H. heidelbergensis* a form of Neandertal. *Homo naledi* clusters with members of the Lubenow Core in at least 84% of the partitions, and *H. georgicus* clusters with members of the Lubenow Core in at least 82% of the partitions. *Homo habilis* clusters with the Lubenow Core in 75% to 80% of the partitions. In contrast, *Homo floresiensis* clusters with the Lubenow Core in only 41% of the partitions but co-occurs in 59% of the partitions with *Homo habilis*. Thus if we choose to include *H. habilis* in the same cluster as the Lubenow Core based on the high frequency with which they cluster together, *Homo floresiensis* might also be included with it but with less confidence. *Homo floresiensis* clusters with outgroup taxa in at most 36% of partitions (with *Au. africanus s.l.*). Finally, we see that *Au. sediba* clusters with *Homo* taxa in at least 55% of the partitions and with *Au. africanus s.l.* and *Au. afarensis* in only 46% and 34% of the partitions respectively.

If we recognize clusters from these partition frequencies based on a simple majority rule, where two taxa belong to the same cluster if they appear together in a cluster in at least 50% of the partitions, we find three clearly-defined clusters. The first cluster contains chimpanzee, gorilla, and *Ardipithecus*. The second cluster contains *Au. afarensis* and *Au. africanus s.l.* The third cluster contains all *Homo* taxa and *Au. sediba*. If we require a more stringent 75% rule, where two taxa belong to the same cluster only if they appear together in a cluster in at least 75% of the partitions, the outgroup clusters are retained, but *Homo floresiensis* no longer belongs to the *Homo* cluster, instead appearing as a taxonomic singleton. *Australopithecus sediba* connects to the *Homo* cluster only by co-occurring in the same cluster as *Homo habilis* in 77% of partitions.

DISCUSSION

Previous results in hominin baraminology using only craniodental characteristics have strongly supported a large human holobaramin that includes unexpected taxa such as *Homo habilis* and *Au. sediba* (Wood 2010, 2016, 2017; Sinclair and Wood 2021). Creationists previously accepted *Homo erectus s.l.*, Neandertals, and *Homo heidelbergensis* as human, but this was based especially on postcranial considerations (Hartwig-Scherer 1998; Lubenow 2004). With *H. naledi* and *Au. sediba* so different from the others postcranially, questions persist about their human status. In the case of *Homo naledi*, cultural evidence of body disposal (Dirks et al. 2010) tentatively confirms their status as human, but with *Au. sediba*, no such supplemental evidence exists and legitimate uncertainty remains.

Here we present a new character matrix of 239 postcranial characters scored for 14 taxa to evaluate the baraminic relationships of hominins. These new characters should aid us in developing a much more holistic perspective on hominin baraminology. Considered alone without craniodental characters, the postcranial characters reveal clustering patterns quite similar to what we have seen repeatedly with different samples of craniodental characters. Unsurprisingly, *Homo sapiens* always clusters together with Neandertals, *Homo heidelbergensis*, *Homo erectus s.l.*, and the Dmanisi hominins. Likewise, chimpanzees, gorillas, and *Ardipithecus* always cluster together and never cluster with *Homo sapiens*. The status of the *Australopithecus* taxa and *H. naledi*, *H. floresiensis*, and *H. habilis* are less clear. Because of the unusual nature of their postcranial skeletons, this should come as no surprise. Distance correlation supports placing *Homo naledi* with other members of *Homo*, which is confirmed by cluster analysis. In contrast, *Australopithecus sediba* sometimes clusters with

Table 2. Frequency of co-clustering. For each pair of taxa, the frequency with which they occur in the same cluster is shown based on 44 different clustering treatments described in this paper.

	Gorilla	Chimpanzee	*Ardipithecus*	*Au. afarensis*	*Au. africanus s.l.*	*Au. sediba*	*H. floresiensis*	*H. georgicus*	*H. habilis*	*H. naledi*	*H. heidelbergensis*	*H. erectus s.l.*	Neandertals	*H. sapiens*
Gorilla	-	100%	100%	34%	27%	5%	9%	0%	0%	0%	0%	0%	0%	0%
Chimpanzee	100%	-	100%	34%	27%	5%	9%	0%	0%	0%	0%	0%	0%	0%
Ardipithecus	100%	100%	-	34%	27%	5%	9%	0%	0%	0%	0%	0%	0%	0%
Au. afarensis	34%	34%	34%	-	89%	34%	30%	18%	21%	21%	18%	18%	18%	18%
Au. africanus s.l.	27%	27%	27%	89%	-	46%	36%	30%	32%	25%	23%	23%	23%	23%
Au. sediba	5%	5%	5%	34%	46%	-	55%	64%	77%	68%	55%	59%	55%	55%
H. floresiensis	9%	9%	9%	30%	36%	55%	-	46%	59%	50%	41%	41%	41%	41%
H. georgicus	0%	0%	0%	18%	30%	64%	46%	-	84%	75%	82%	86%	82%	82%
H. habilis	0%	0%	0%	21%	32%	77%	59%	84%	-	91%	75%	80%	75%	75%
H. naledi	0%	0%	0%	21%	25%	68%	50%	75%	91%	-	84%	89%	84%	84%
H. heidelbergensis	0%	0%	0%	18%	23%	55$	41%	82%	75%	84%	-	96%	100%	100%
H. erectus s.l.	0%	0%	0%	18%	23%	59%	41%	86%	80%	89%	96%	-	96%	96%
Neandertals	0%	0%	0%	18%	23%	55%	41%	82%	75%	84%	100%	96%	-	100%
H. sapiens	0%	0%	0%	18%	23%	55%	41%	82%	75%	84%	100%	96%	100%	-

other *Australopithecus* species and sometimes clusters with no other taxa in the distance correlation results.

What should we make of these results? First, the inconsistency between clustering methods does not seem unique to the postcranial characters, since we see the same inconsistencies when using the full craniodental set or the high relevance ($a \geq 0.5$) craniodental characters. In our previous work, we found more consistency with the full craniodental set and a slightly larger taxon sample, suggesting that the present taxon sample may still be too small to reveal reliable clusters. Ideally, cluster analyses work best when there are well-defined clusters with multiple points in each. In many of the cases we present here, a possible cluster is accompanied by a heterogeneous set of outlying points that do not form a single cluster. This is not ideal for cluster analysis. Ironically, it may be further discoveries of nonhuman ape taxa that help to clarify the boundaries of humanity.

Despite these inconsistencies, when we look at the frequency with which taxon pairs cluster together in our partitions, we can see fairly clear trends. There is a group of *Homo* taxa, excluding *Homo floresiensis*, that almost always cluster together. This group includes *H. naledi*, *H. sapiens*, *H. neanderthalensis*, *H. erectus s.l.*, and *H. heidelbergensis*. Not surprisingly, the evidence for cultural sophistication is strongest here (Ross et al. 2023), and we suggest these taxa can be accepted as Near Certain Humans (or certain in the case of *Homo sapiens*) (NCH).

Surprisingly, despite cultural evidence that *Homo floresiensis* is human (Wise 2005), it clusters with NCH in an average of only 45.5% of the partitions. In past craniodental analyses, we have also seen *Homo floresiensis* not clustering with other *Homo* taxa, but since the known character states for *H. floresiensis* amounted to only 32.2% of the full craniodental character set, we speculated that the paucity of data artifactually separated *H. floresiensis* from other human taxa. Here, 60.3% of the postcranial characters are scored for *H. floresiensis*, and we still do not see a close clustering of *H. floresiensis* with other *Homo* taxa. We thus must consider the likelihood that *H. floresiensis* differs anatomically from other humans or might exhibit developmental pathologies, as suggested by Rupe and Sanford (2017). Still, with the combined character set of 482 characters, *Homo floresiensis* clusters with other *Homo* taxa in all distance correlation partitions, all medoid partitioning, and in the two-cluster fuzzy analysis.

Our postcranial characters generate a greater degree of uncertainty regarding the status of *Au. sediba*. In the present craniodental analyses and in previous studies *Au. sediba* has always clustered with *Homo* taxa (except for *H. floresiensis*), but with the postcranial characters *Au. sediba* clusters with no other taxa or with other australopiths. This is not surprising since the postcranial skeleton is known to differ considerably from NCH like *H. sapiens*, *H. erectus s.l.*, and *H. neanderthalensis*. With 72.4% of *Au. sediba*'s postcranial character states scored, this clustering is unlikely to be a statistical artifact. With the combined craniodental and postcranial characters, *Au. sediba* clusters consistently with *Homo* taxa again, as it does with the craniodental characters alone. This difference between clustering with postcranial characters versus the combined character set cannot be attributed to a bias towards craniodental characters, because only 49% of *Au. sediba*'s craniodental characters are scored. If anything, the combined character set should reflect a bias towards postcranial

characters and should therefore continue to show *Au. sediba* separated from *Homo*. Thus, we might cautiously interpret our present results as consistent with previous classifications of *Au. sediba* as human.

An alternative perspective on *Au. sediba* might invoke some form of neoteny or paedomorphosis to argue that juvenile australopiths might more closely resemble adult *Homo* than mature australopiths. If that is the case, it is possible that the craniodental characteristics exaggerate the resemblance between *Au. sediba* and *Homo* because the principal source of cranial information from *Au. sediba* is a juvenile skull. Thus, when considering craniodental characters alone, *Au. sediba* closely clusters with members of *Homo*, while examination of postcranial characters creates more of a division between *Homo* and *Australopithecus*, including *Au. sediba*. A complete adult skull might support placing *Au. sediba* outside of the human holobaramin. While this is an interesting possibility, it does not account for the fact that *Au. sediba* appears in the *Homo* cluster with the combined data (Figures 10 and 11), where the known postcranial characters outnumber the known craniodental characteristics. At this point, a mature *Au. sediba* skull is likely needed to resolve these questions.

Future research on hominin baraminology ought to focus on improving our sample of characters and character states as well as expanding methodologically into morphometrics. While the craniodental and postcranial characters have roughly the same proportion of characters scored (61.9% and 65.7% respectively), the individual taxa vary considerably in their taxic relevance. For example, chimpanzees, gorillas, and *Homo sapiens* have taxic relevance of only 0.749, 0.798, and 0.893 for the full craniodental character matrix, which is unnecessary. Similarly, Neandertals have a taxic relevance of only 0.621 for the full craniodental set, despite the existence of many well-documented and accessible skulls. The craniodental character matrix could readily be filled out to a much greater extent, which would theoretically provide a much better understanding of the human holobaramin based on craniodental characters.

At the same time, additional postcranial characters could be generated, especially when information about the Little Foot skeleton becomes more readily accessible. With the relative completeness of the Little Foot skeleton, the postcranial taxic relevance of *Au. africanus s.l.* should increase to near 1, but the skeleton is presently unreconstructed and mostly unavailable in public 3D scanning databases. We were able to glean only limited information from the published descriptions and photographs of the skeleton. Additional efforts could also be made to fill out the *Au. afarensis* character states. We were able to evaluate a second generation cast of AL 288-1, as well as casts of material from AL 333, but information on the Dikika juvenile and adult Kadanuumuu skeletons is less accessible.

Finally, morphometrics has been applied only sparingly in baraminology but may represent an important methodological addition to our toolkit. If informal human cognition represents an important ingredient in identifying baramins (Sanders and Wise 2003), then cognition operates primarily on the basis of shape and form rather than individual occurrence of characters. Due to the widespread availability of discrete character-based data used for phylogenetic analyses, discrete character-based methods have dominated baraminology for twenty years. Serious efforts should be made to expand to the study of form and shape, which can be afforded by morphometrics.

ACKNOWLEDGEMENTS

This research was supported by a grant from the Genesis Fund and by donor gifts to Core Academy of Science. A Sanders Scholarship to P.S.B. also helped support our work. We are grateful to Lucinda Hill and Southern Adventist University for providing access to the cast skeletons of chimpanzee and gorilla in their collection.

REFERENCES

Alemseged, Z., F. Spoor, W.H. Kimbel, R. Bobe, D. Geraads, D. Reed, and J.G. Wynn. 2006. A juvenile early hominin skeleton from Dikika, Ethiopia. *Nature* 443:296–301. DOI: 10.1038/nature05047.

Argue, D., C.P. Groves, M.S.Y. Lee, and W.L. Jungers. 2017. The affinities of *Homo floresiensis* based on phylogenetic analyses of cranial, dental, and postcranial characters. *Journal of Human Evolution* 107:107–133. DOI: 10.1016/j.jhevol.2017.02.006.

Arsuaga, J.L., J.-M. Carretero, C. Lorenzo, A. Gómez-Olivencia, A. Pablos, L. Rodríguez, R. García-González, A. Bonmatí, R.M. Quam, A. Pantoja-Pérez, I. Martínez, A. Aranburu, A. Gracia-Téllez, E. Poza-Rey, N. Sala, N. García, A. Alcázar de Velasco, G. Cuenca-Bescós, J.M. Bermúdez de Castro, and E. Carbonell. 2015. Postcranial morphology of the middle Pleistocene humans from Sima de los Huesos, Spain. *Proceedings of the National Academy of Sciences* 112:11524–11529. DOI: 10.1073/pnas.1514828112.

Berger, L.R., D.J. De Ruiter, S.E. Churchill, P. Schmid, K.J. Carlson, P.H.G.M. Dirks, and J.M. Kibii. 2010. *Australopithecus sediba*: A new species of *Homo*-like australopith from South Africa. *Science* 328:195–204. DOI: 10.1126/science.1184944.

Berger, L.R., J. Hawks, D.J. De Ruiter, S.E. Churchill, P. Schmid, L.K. Delezene, T.L. Kivell, H.M. Garvin, S.A. Williams, J.M. DeSilva, M.M. Skinner, C.M. Musiba, N. Cameron, T.W. Holliday, W. Harcourt-Smith, R.R. Ackermann, M. Bastir, B. Bogin, D. Bolter, J. Brophy, Z.D. Cofran, K.A. Congdon, A.S. Deane, M. Dembo, M. Drapeau, M.C. Elliott, E.M. Feuerriegel, D. Garcia-Martinez, D.J. Green, A. Gurtov, J.D. Irish, A. Kruger, M.F. Laird, D. Marchi, M.R. Meyer, S. Nalla, E.W. Negash, C.M. Orr, D. Radovcic, L. Schroeder, J.E. Scott, Z. Throckmorton, M.W. Tocheri, C. VanSickle, C.S. Walker, P. Wei, and B. Zipfel. 2015. *Homo naledi*, a new species of the genus *Homo* from the Dinaledi Chamber, South Africa. *eLife* 4:e09560. DOI: 10.7554/eLife.09560.

Berger, L.R., and J. Hawks. 2019. *Australopithecus prometheus* is a *nomen nudum*. *American Journal of Physical Anthropology* 168:383–387. DOI: 10.1002/ajpa.23743.

Churchill, S.E., and C. VanSickle. 2017. Pelvic morphology in *Homo erectus* and early *Homo*. *The Anatomical Record* 300:964–977. DOI: 10.1002/ar.23576.

Clarke, R.J. 2019a. Excavation, reconstruction and taphonomy of the StW 573 *Australopithecus prometheus* skeleton from Sterkfontein Caves, South Africa. *Journal of Human Evolution* 127:41–53. DOI: 10.1016/j.jhevol.2018.11.010.

Clarke, R.J. 2019b. *Australopithecus prometheus* was validly named on MLD 1. *American Journal of Physical Anthropology* 170:479–481. DOI: 10.1002/ajpa.23892.

DeWitt, D.A. 2010. Baraminological analysis places *Homo habilis*, *Homo rudolfensis*, and *Australopithecus sediba* in the human holobaramin: discussion. *Answers Research Journal* 3:156–158.

Dirks, P.H.G.M., L.R. Berger, E.M. Roberts, J.D. Kramers, J. Hawks, P.S. Randolph-Quinney, M. Elliott, C.M Musiba, S.E Churchill, D.J. De Ruit-

er, P. Schmid, L.R Backwell, G.A Belyanin, P. Boshoff, K.L. Hunter, E.M Feuerriegel, A. Gurtov, J. Du G. Harrison, R. Hunter, A. Kruger, H. Morris, T.V. Makhubela, B. Peixotto, and S. Tucker. 2010. Geological and taphonomic context for the new hominin species *Homo naledi* from the Dinaledi Chamber, South Africa. *eLife* 4:e09561. DOI: 10.7554/eLife.09561.

Grine, F.E. 2019. The alpha taxonomy of *Australopithecus* at Sterkfontein: The postcranial evidence. *Comptes Rendus Palevol* 18:335–352. DOI: 10.1016/j.crpv.2019.01.004.

Groening, F., G-C. Weniger, and J.F. Kegler. 2007. The digital world of Neanderthals - NESPOS, an online archive for Neanderthal research. *Archaologisches Korrespondenzblatt* 37, no. 3:321–333.

Habermehl, A. 2010. Baraminological analysis places *Homo habilis*, *Homo rudolfensis*, and *Australopithecus sediba* in the human holobaramin: discussion. *Answers Research Journal* 3:155–156.

Haile-Selassie, Y., B.M. Latimer, M. Alene, A.L. Deino, L. Gibert, S.M. Melillo, B.Z. Saylor, G.R. Scott, and C.O. Lovejoy. 2010. An early *Australopithecus afarensis* postcranium from Woranso-Mille, Ethiopia. *Proceedings of the National Academy of Sciences* 107:12121–12126. DOI: 10.1073/pnas.1004527107.

Hartwig-Scherer, S. 1998. Apes or ancestors? Interpretations of the hominid fossil record within evolutionary and basic type biology. In W.A. Dembski (editor), *Mere Creation*, pp. 212–235. Downers Grove, Illinois: InterVarsity Press.

Kivell, T.L., J.M. Kibii, S.E. Churchill, P. Schmid, and L.R. Berger. 2011. *Australopithecus sediba* hand demonstrates mosaic evolution of locomotor and manipulative abilities. *Science* 333:1411–1417. DOI: 10.1126/science.1202625.

Lordkipanidze, D., T. Jashashvili, A. Vekua, M.S. Ponce De León, C.P.E. Zollikofer, G.P. Rightmire, H. Pontzer, R. Ferring, O. Oms, M. Tappen, M. Bukhsianidze, J. Agusti, R. Kahlke, G. Kiladze, B. Martinez-Navarro, A. Mouskhelishvili, M. Nioradze, and L. Rook. 2007. Postcranial evidence from early *Homo* from Dmanisi, Georgia. *Nature* 449:305–310. DOI: 10.1038/nature06134.

Lubenow, M.L. 2004. *Bones of Contention: A Creationist Assessment of Human Fossils*, revised ed. Grand Rapids, Michigan: Baker Books.

Marchi, D., C.S. Walker, P. Wei, T.W. Holliday, S.E. Churchill, L.R. Berger, and J.M. DeSilva. 2017. The thigh and leg of *Homo naledi*. *Journal of Human Evolution* 104:174–204. DOI: 10.1016/j.jhevol.2016.09.005.

Menton, D.N. 2010. Baraminological analysis places *Homo habilis*, *Homo rudolfensis*, and *Australopithecus sediba* in the human holobaramin: discussion. *Answers Research Journal* 3:153–155.

O'Micks, J. 2016. *Homo naledi* probably not part of the human holobaramin based on baraminic re-analysis including postcranial evidence. *Answers Research Journal* 9:263–272.

O'Micks, J. 2017a. Rebuttal to "Reply to O'Micks concerning the geology and taphonomy of the *Homo naledi* site" and "Identifying humans in the fossil record: A further response to O'Micks." *Answers Research Journal* 10:63–70.

O'Micks, J. 2017b. Further evidence that *Homo naledi* is not a member of the human holobaramin based on measurements of vertebrae and ribs. *Answers Research Journal* 10:103–113.

Pugh, K.D. 2022. Phylogenetic analysis of Middle-Late Miocene apes. *Journal of Human Evolution* 165:103140. DOI: 10.1016/j.jhevol.2021.103140.

Reeves, C.R. 2021a. A critical evaluation of statistical baraminology: Part 1—Statistical principles. *Answers Research Journal* 14:261–269.

Reeves, C.R. 2021b. A critical evaluation of statistical baraminology: Part 2—Alternatives and conceptual and practical issues. *Answers Research Journal* 14:271–282.

Ross, M. R., P.S. Brummel, and T.C. Wood. 2023. Human history from Adam to Abraham: Integrating paleoanthropology with a young-age creation perspective In J.H. Whitmore (editor), *Proceedings of the Ninth International Conference on Creationism*, pp. 66-87. Cedarville, Ohio: Cedarville University International Conference on Creationism.

Rupe, C., and J. Sanford. 2017. *Contested Bones*. Canandaigua, New York: FMS Publications.

Sanders, R., and K.P. Wise. 2003. The cognitum: a perception-dependent concept needed in baraminology. In R.L. Ivey, Jr. (editor), *Proceedings of the Fifth International Conference on Creationism*, pp. 445–456. Pittsburgh, Pennsylvania: Creation Science Fellowship.

Senter, P. 2010. Were australopithecines ape-human intermediates or just apes? A test of both hypotheses using the "Lucy" skeleton. *The American Biology Teacher* 72, no. 2:70–76. DOI: 10.1525/abt.2010.72.2.4.

Sinclair, P., and T.C. Wood. 2021. Revising hominin baraminology with medoid partitioning and fuzzy analysis. *Answers Research Journal* 14:451–462.

Wise, K.P. 2005. The Flores skeleton and human baraminology. *Occasional Papers of the BSG* 6:1–13.

Wood, T.C. 2010. Baraminological analysis places *Homo habilis*, *Homo rudolfensis*, and *Australopithecus sediba* in the human holobaramin. *Answers Research Journal* 3:71–90.

Wood, T.C. 2013. *Australopithecus sediba*, statistical baraminology, and challenges to identifying the human holobaramin. In M. Horstemeyer (editor), *Proceedings of the Seventh International Conference on Creationism*, article 16. Pittsburgh, Pennsylvania: Creation Science Fellowship.

Wood, T.C. 2016. An evaluation of *Homo naledi* and "early" *Homo* from a young-age creationist perspective. *Journal of Creation Theology and Science Series B: Life Sciences* 6:14–30.

Wood, T.C. 2017. Identifying humans in the fossil record: A further response to O'Micks. *Answers Research Journal* 10:57–62.

Wood, T. 2020. An expanded character set for evaluating the phylogenetic position of *Homo floresiensis*. In S.R. Leigh (editor), *Program of the 89th Annual Meeting of the American Association of Physical Anthropologists April 15–18, 2020*, p. 312. Los Angeles: American Association of Physical Anthropologists.

Wood, T.C. 2021. Baraminology by cluster analysis: A response to Reeves. *Answers Research Journal* 14:283–302.

Wood, T.C., and P.S. Brummel. 2023. Postcranial characters for analyzing hominin relationships and adaptations. Retrieved April 28, 2023, from https://doi.org/10.5061/dryad.tb2rbp05f.

THE AUTHORS

Todd Charles Wood is a researcher, teacher, and lecturer with twenty years' experience working in young-age creationism. He is especially known for his studies of created kinds and fossil hominins. He is currently president of Core Academy of Science and resides in Dayton, Tennessee, home of the Scopes Trial.

PS Brummel is a student and hominin fossil aficionado. He was awarded the 2022 Sanders Scholarship from Core Academy of Science. He currently resides in Indiana.